Kinetics of Multiplex Hybridization: Mechanisms and Implications

J. Bishop, A. M. Chagovetz, and S. Blair
Electrical and Computer Engineering, University of Utah, Salt Lake City, Utah

ABSTRACT Quantitative analysis of DNA microarray data is complicated by uncertainties inherent to the experimental setup. Using computer simulations and real-time experimental results, we have previously demonstrated effects of multiplex reactions on a single sensing zone of an array, which may be a leading factor in erroneous interpretation of experimental data. We suggest here that a simplified three-component kinetic model may present a sufficient approximation to describe the general case of DNA sensing in a complex sample milieu. We show that, by analyzing the real-time hybridization kinetics of a nontarget species, we can perform quantitative analysis of unlabeled targets of interest within a broad dynamic range of concentrations.

INTRODUCTION

Use of DNA microarray-based analysis has quickly expanded in genetic research and in various genomic applications since its introduction in the early 1990s (1). Indeed, microarrays offer geneticists the opportunity to analyze massive amounts of data (up to the whole genome) in the course of a single experiment. The primary goal of microarray-based methodologies is to answer two basic questions: what, and how much; i.e., to determine the quantitative and qualitative (sequence-specific) composition of nucleic acids in the sample). There exists, however, a significant discrepancy of opinions between the general scientific public who often perceive DNA microarrays as established analytical tools and practitioners who have legitimate concerns about the reliability of microarray data (2–5).

The major efforts in primary data analysis are dedicated to developing robust statistical algorithms, which interpret large masses of data, and in assigning biological significance to experimental results (6). Statistical problems are significant because the sampling of fluorescent signals is done only once in the course of experiment (i.e., end-point readout), so that hundreds of thousands of independent variables are analyzed based on a few data points per each (depending on the degree of replication). In parallel, several groups have undertaken studies targeting the numerous physical and chemical processes in play, which define the limitations of current technology, and have critical impact on the interpretation of data. Problems associated with these limitations need to be resolved to bring microarrays to the level of a true analytical tool. We suggest that these problems can be grouped into four clusters: sample preparation; surface chemistry; mass transport; and molecular recognition.

Sample preparation includes a multitude of methods of extraction of nucleic acids from biological samples, shearing of nucleic acids, amplification and labeling (or lack thereof), and generating single stranded targets. Each processing step is a potential source of quantitative bias in experimental results (7), where the ideal paradigm calls for minimizing preparatory steps. Although there are efforts to standardize sample preparation procedures (8), it is difficult to foresee a universally accepted protocol that is equally applicable to all microarray experiments.

Surface chemistry has to provide predictable and reproducible attachment of DNA probes to the surface. Major parameters affecting surface chemistry are characteristics of the surface proper: roughness, hydrophobicity, density of chemical functionalities and charges; chemistry of linking probes; density and orientation of probes; size and geometry of the spots; and microarray architecture. All these factors have significant effects on the kinetics of hybridization, and on the results of microarray experiments (9,10).

DNA sensing occurs on the liquid-solid interface and two major processes determine the apparent rate of target capture: mass transport of the targets to the sensing surface and kinetics of surface hybridization (11,12). Mass transport effects play a crucial role in microarray experiments, especially if the targets are present in low abundance. Under target limiting conditions, lateral diffusion of targets to the sensing spot and vertical diffusion to the surface become rate-limiting. In addition, the creation of local depletion zones modulates the specificity of capture and can lead to quantification biases (4,10). Experimental study of hybridization kinetics in multicomponent systems indicates continuing growth of surface concentration of specific targets after 72 h (13), so equilibrium analysis of microarray data should be used with caution. Active delivery methods have been proposed to enhance mass transport (14–17), some of which are implemented in commercial instruments. Even though mass transport enhancements reduce the time to equilibrium, they are less efficient in the complex environment, where the competitive displacement mechanism may become rate-limiting (17,18).

Molecular recognition problems revolve around a common theme: the inherent cross-hybridization of targets due to

Submitted September 6, 2007, and accepted for publication October 18, 2007.

Address reprint requests to S. Blair, E-mail: blair@ece.utah.edu.

Editor: Jonathan B. Chaires.

0006-3495/08/03/1726/09 $2.00

doi: 10.1529/biophysj.107.121459

imperfect capture specificity. Cross-hybridization is responsible for multiple reactions between heterogeneous DNA sequences as well as partitioning of targets across multiple sensing zones, i.e., multiple targets hybridizing to one zone and one target hybridizing to multiple zones. These effects are compounded due to the growing size of arrays. The importance of reaching equilibrium on DNA microarrays is also well recognized (19); equilibrium insures temporal stability of the signal and maximal discrimination between a target and nontarget species (20), which are thermodynamically predictable (21,22). Indeed, cross-hybridization and nonequilibrium conditions have been implicated as mechanisms affecting the interpretation of microarray results (19,23). Analysis of published data suggested that ~75% sequence homology is required to cause significant cross-hybridization; subsequent analysis of probes on multiple commercial arrays showed that some of them produce a large number of false positives due to cross-hybridization (24). A review of some of the arrays offered by Affymetrix (Santa Clara, CA) showed that cross-hybridization may affect a major part of the logged data (25).

Even for a simple two-component scenario, hybridization signals display complex nonmonotonic behavior due to competitive displacement interactions (20,22,26), which depend on the relative affinities, concentrations of the components, temperature, and mass transport mechanisms. Effects of secondary structure also need to be addressed in this context, especially when they are associated with small sequence alterations: SNPs, deletions, and insertions. A general theoretical approach to describe multiple solution- and surface-based reactions during hybridization experiments has been developed (22), but its full complexity has not yet been studied.

There are several perspectives for addressing molecular recognition problems. The currently accepted approaches are based on thermodynamics, the practical implication of which lies in the optimized design of the surface probe sequences and bulk experimental conditions to minimize cross hybridizations: ionic strength, buffer composition, and temperature. A necessary requirement for applying the thermodynamic approach in data analysis is the equilibrium state of the surface reactions, which in general is not achieved (the degree of completion of hybridization may vary considerably depending on the instrumental platform used). Another approach is to elucidate kinetic mechanisms of multiplex reactions and apply kinetic analysis to extract quantitative information (11,27). This approach relies on thermodynamic methods for probe design and optimization of experimental conditions, but in contrast, the analysis uses real-time hybridization curves, which eliminates equilibrium assumptions. In addition, the analysis no longer assumes perfect molecular recognition and therefore accounts directly for the problem of cross-hybridization.

We suggest that the kinetic approach, which requires a paradigm shift in microarray experimentation, may resolve many issues associated with molecular recognition in complex samples. In fact, we (28,29) and others (4) have experimentally demonstrated the time-course of competitive displacement phenomena in multiplex environments, with excellent agreement to simulation results. Although sequence-specific effects have not been addressed explicitly in our work, it is implicitly understood that sequence effects are reflected in the corresponding rate constants (30) (in the approximation used here, the dissociation rate constants).

Here we study how changes in sample composition modify the kinetics of hybridization. Using a multicomponent kinetic model of hybridization, in which the hybridization of all DNA sequences to a single sensing zone are intertwined, we perform simulations varying the number and concentration of DNA species. We show that, even in this complex environment, the kinetics of hybridization can be adequately described by considering only three components—the perfectly matched target, a high affinity nontarget (competitor), and low affinity nontarget (apparent background). This approximation significantly simplifies the development of analysis methods. We then extend the simulation work to an experimental setup where we track the hybridization kinetics of the competitor species in real-time and show how it is affected by the presence of a perfectly matched target plus two background species with small sequence variation and varying concentrations. Using both simulation and experimental results, we extend the discussion from the effects of cross-hybridization of background species to the use of the real-time hybridization curve of the competitor to quantitatively assess the concentration of a perfectly matched target under nonequilibrium conditions in the context of the three-component model, even in the presence of multiple background species.

THEORY

We consider a simplification to the more general model of the chemical reaction of N different species to a single probe species (22,20),

$$\frac{dB_i(t)}{dt} = k_{a,i}C_i(t)\left[R_T - \sum_{j=1}^{N} B_j(t)\right] - k_{d,i}B_i(t), \qquad (1)$$

where $B_i(t)$ represents bound surface concentrations, $k_{a,i}$ the association rate constant for each reaction, $C_i(t)$ the solution concentration, R_T the concentration of probe, and $k_{d,i}$ the dissociation rate constants. This environment is one in which all species can compete for the same probe site, but at equilibrium the highest affinity species will partially displace all others, with dynamic range at equilibrium determined by the relative dissociation rates and concentrations of species (20). Our model disregards surface-specific effects: electrostatic repulsion and probe accessibility (31,32). We also disregard relative target to probe orientation and its effects on nucleation rates (33) as well as cross-hybridization of targets in

solution (22) and secondary structure effects (34) (although the latter effects may be described by the use of effective concentrations (28)). This model can be readily extended to include these effects, but our simplification is sufficient to study the essential features of competition in multiplex hybridization.

In a typical experiment with end-point measurement, the quantity being measured at each spot is total fluorescence

$$F(t) = c\sum_{\mathrm{i}=1}^{\mathrm{N}} B_{\mathrm{i}}(t), \tag{2}$$

where t is the hybridization time, c is a proportionality constant, and it is assumed that all species are identically fluorescently labeled. In a real-time experiment, $F(t)$ is measured continuously at discrete time points.

Mass transport can reasonably be incorporated using the two-compartment model, where the concentration $C_{\mathrm{i}}(t)$ in the lower compartment is described by (35,36)

$$\frac{V}{S}\frac{dC_{\mathrm{i}}(t)}{dt} = -k_{\mathrm{a,i}}C_{\mathrm{i}}(t)\left[R_{\mathrm{T}} - \sum_{\mathrm{j}=1}^{\mathrm{N}} B_{\mathrm{j}}(t)\right] + k_{\mathrm{d,i}}B_{\mathrm{i}}(t) + k_{\mathrm{M}}[C_{\mathrm{i}} - C_{\mathrm{i}}(t)], \tag{3}$$

where the C_{i} values represent constant concentrations in the upper compartment, V is the volume of the lower compartment, S is the surface area intersecting the two compartments, and k_{M} represents the diffusion of target across the interface.

It should be clear that the kinetics of all species involved is interdependent through competition for the probe sites. However, it should also be clear that using this model for the interpretation of microarray data can quickly become an intractable problem as the number of interacting species increases. In addition, the model requires some estimation of kinetic rate constants and concentrations of all species involved, which generally are not known a priori, although rate constants can be obtained from sequence-specific calculations (4).

As a simplified basis for analysis of microarray data, we also consider a simplified three-component model consisting of the complementary target, the highest affinity mismatch (a competitor), and a composite of all other interacting species with lower affinity (background),

$$\frac{dB_{\mathrm{t}}}{dt} = k_{\mathrm{a,t}}C_{\mathrm{t}}(t)[R_{\mathrm{T}} - B_{\mathrm{t}}(t) - B_{\mathrm{c}}(t) - B_{\mathrm{b}}(t)] - k_{\mathrm{d,t}}B_{\mathrm{t}}(t), \tag{4}$$

$$\frac{dB_{\mathrm{c}}}{dt} = k_{\mathrm{a,c}}C_{\mathrm{c}}(t)[R_{\mathrm{T}} - B_{\mathrm{t}}(t) - B_{\mathrm{c}}(t) - B_{\mathrm{b}}(t)] - k_{\mathrm{d,c}}B_{\mathrm{c}}(t), \tag{5}$$

$$\frac{dB_{\mathrm{b}}}{dt} = k_{\mathrm{a,b}}C_{\mathrm{b}}(t)[R_{\mathrm{T}} - B_{\mathrm{t}}(t) - B_{\mathrm{c}}(t) - B_{\mathrm{b}}(t)] - k_{\mathrm{d,b}}B_{\mathrm{b}}(t), \tag{6}$$

where the appropriate modifications of the lower compartment concentrations also need to be made.

MATERIALS AND METHODS

Simulation

We will use the analytical description of multiplex hybridization described in the previous section to perform virtual experiments with $N \leq 7$. We assume that the association rates of all the species are equal (37), with value $10^6\ \mathrm{M}^{-1}\ \mathrm{s}^{-1}$. The dissociation rate for the primary target is set to $k_{\mathrm{d,t}} = 4.55 \times 10^{-6}\ \mathrm{s}^{-1}$, the competitor is $k_{\mathrm{d,c}} = 5 \times 10^{-4}\ \mathrm{s}^{-1}$, and the background dissociation rates range from $7.5 \times 10^{-4}\ \mathrm{s}^{-1}$ to $3.67 \times 10^{-2}\ \mathrm{s}^{-1}$. This range was chosen to simulate increasingly unstable targets. It should be pointed out that the dissociation rate constants and association rate constants chosen for the simulations are the same ones used during the fitting of the experimental data. Additionally, the probe concentration R_{T} is set to 10^{-11} Mm for the simulations and allowed to vary during the fit of experimental data. However, R_{T} stayed within the range of 1×10^{-11} to 5×10^{-11} for all fits. In addition, the coefficient representing diffusion between the upper and lower compartments, k_{M}, is set to 10^{-6} cm/s.

Simulations were performed by implementing custom code in MATLAB (The MathWorks, Natick, MA). The function ode15s was used as a differential equation solver. In performing the fits with the $N = 3$ model, the fminsearch optimization routine was used.

Experimental

We use mixtures of four different 20-mer sequences: a target of interest (5′ to 3′ CGAGG GCAGCAATAGTACAC, perfect complement to the probe), a competitor (Cy-3 CGAGG GCAGCATTAGTACAC), a tandem mismatch (CGAGGGCAGCATAAGTACAC), and a three-base deletion plus insertion (CGAGGGCAGCAGTACACTTT). Only the competitor sequence is fluorescently labeled, and is therefore the only sequence detected by our fluorescence reader. In a previous article (29), we showed that it is sufficient to monitor the kinetics of the competitor to assess the presence and concentration of the target sequence, hence allowing label-free detection of the target.

Real-time experiments are performed using a custom-built fluorescence detection setup (28). A 532-nm laser was end-fire-coupled into a quartz microscope slide which served as an optical waveguide and therefore produced an evanescent field responsible for fluorescence excitation at the surface. The slide also served as our sensing surface where immobilized probe sites are located and where hybridization takes place. The microscope slide is fixed to a custom heating unit that uses a computer-controlled Peltier heater to adjust the temperature of the hybridization. All experiments are performed at 30°C. A hybridization chamber was made by applying a PDMS gasket to the quartz slide. After dispensing the hybridization solution into the inner boundary of the gasket, a glass slide is then placed on top of the gasket to complete the chamber. Using a CCD camera (ST-7XMEI; Santa Barbara Instrument Group, Santa Barbara, CA) mounted above the sensing surface, a time-dependent fluorescence signal, proportional to $B_{\mathrm{c}}(t)$, is detected. Each frame captured by the camera is exposed for 2.5 s and then saved for postprocessing. A digital output signal from the camera shutter is used to modulate the laser output to reduce photobleaching during the time interval between acquisitions. Further experimental details, such as surface modification chemistry, target and probe preparation, probe immobilization, and normalization, can be found in the literature (28,29). Note one difference from the referenced procedure is the slides used for this article had the GPS layer deposited by Yield Engineering (San Jose, CA).

RESULTS

Simulations

We begin with $N = 4$ components to illustrate the kinetics of multicomponent hybridization: target, competitor, and two

background species. Dissociation rates for the two background species are $k_d = 7.5 \times 10^{-4}\ s^{-1}$ and $k_d = 4.63 \times 10^{-3}\ s^{-1}$. Fig. 1 shows the individual hybridization curves, along with the composite hybridization curve that would be observed assuming that all species are detected equally; it is clear that the composite curve gives very little indication as to the hybridization kinetics of the target species. To be consistent with other graphs, all hybridization curves are normalized against the maximum hybridization signal produced by the competitor species alone.

The hybridization curve of the target always increases monotonically; since the target is at a lower concentration than other species, it does not control the initial phase of hybridization (in this case, the competitor and low-affinity background control). In the presence of the target, the competitor will always be displaced (as shown here), while in the absence of the target, the competitor will be the highest affinity species and monotonically increase. As shown in the plot, the background species are displaced, but with very different kinetics. The low affinity background is at higher concentration, so it initially grows rapidly, but, because of its low affinity, it is quickly displaced. However, the high affinity background (at lower concentration) grows more slowly and is displaced more slowly. Even in a complex environment, the equilibrium distribution can be predicted via thermodynamic models, but it is not practical to measure experimentally. In the kinetic regime, the distribution of bound species is time-dependent, as should be clear here. Also shown in the figure is the composite background signal as determined by fitting with the three-component model.

We now investigate how background hybridization affects the kinetics of the target and competitor. Fig. 2 shows the target and competitor hybridization curves as the target is added to the sample and as the number of background species increases from 0 to 5; the dissociation rates of the background increase from $7.5 \times 10^{-4}\ s^{-1}$ for the first background species to $3.67 \times 10^{-2}\ s^{-1}$ for the fifth. These results indicate dramatic effects on the hybridization kinetics of the target and competitor as reflected in the decrease in their bound concentrations. However, the influence on kinetics diminishes as the affinity of the background species decreases, i.e., there is very little change as the fifth background is added, suggesting that cross-hybridization diminishes significantly for species with high dissociation rates (for a fixed concentration).

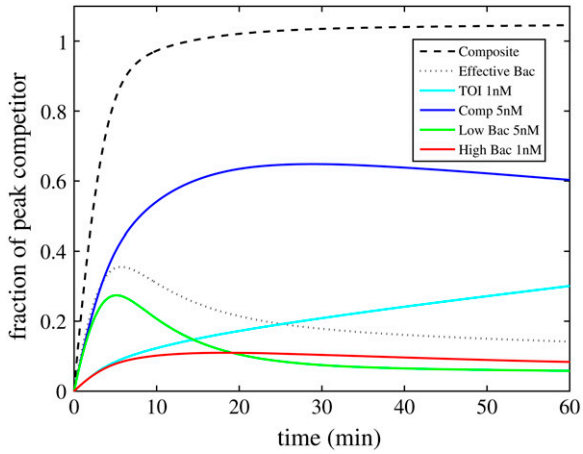

FIGURE 1 Simulated hybridization curves for a multiplex hybridization with four components: target, competitor, and high and low background species. The composite curve (sum of all components) and effective background are also shown.

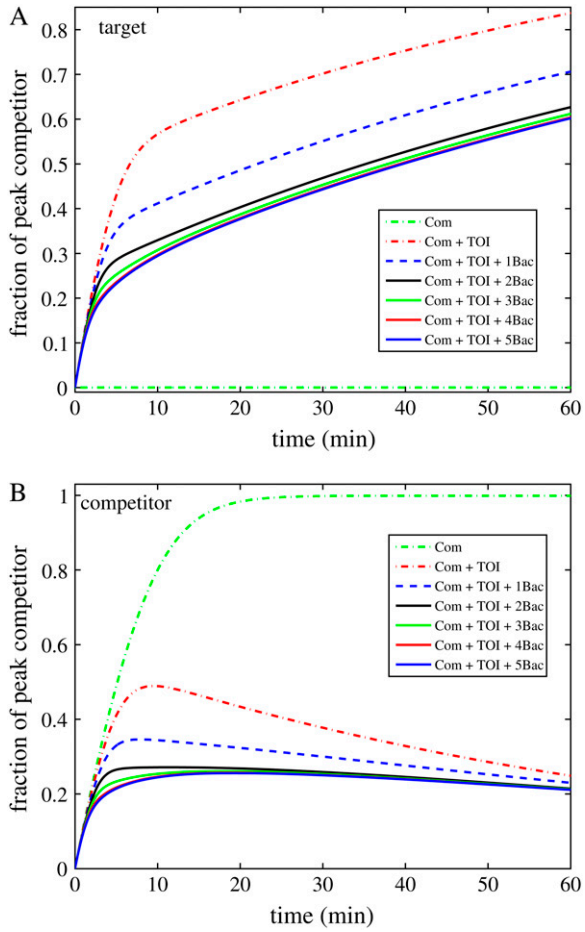

FIGURE 2 Hybridization curves representing the (*A*) target and (*B*) competitor kinetics as the number of background species increases from 0 to 5. Each progressive background species has a larger k_d value to simulate decreasing stability. All species are present at 5-nM concentrations.

Using these five background species, simulations were performed to study how a change in the concentration of the high-affinity background species ($k_d = 7.5 \times 10^{-4}\ s^{-1}$; see Fig. 3, *A* and *B*) and the low-affinity background species ($k_d = 4.63 \times 10^{-3}\ s^{-1}$; see Fig. 3, *C* and *D*) affect the target and competitor. Two different target concentrations are shown (1 nM and 5 nM). These results show that as the concentration of the target increases, the hybridization rate of the competitor decreases rapidly. As the concentration of the high affinity background species increases, both the target

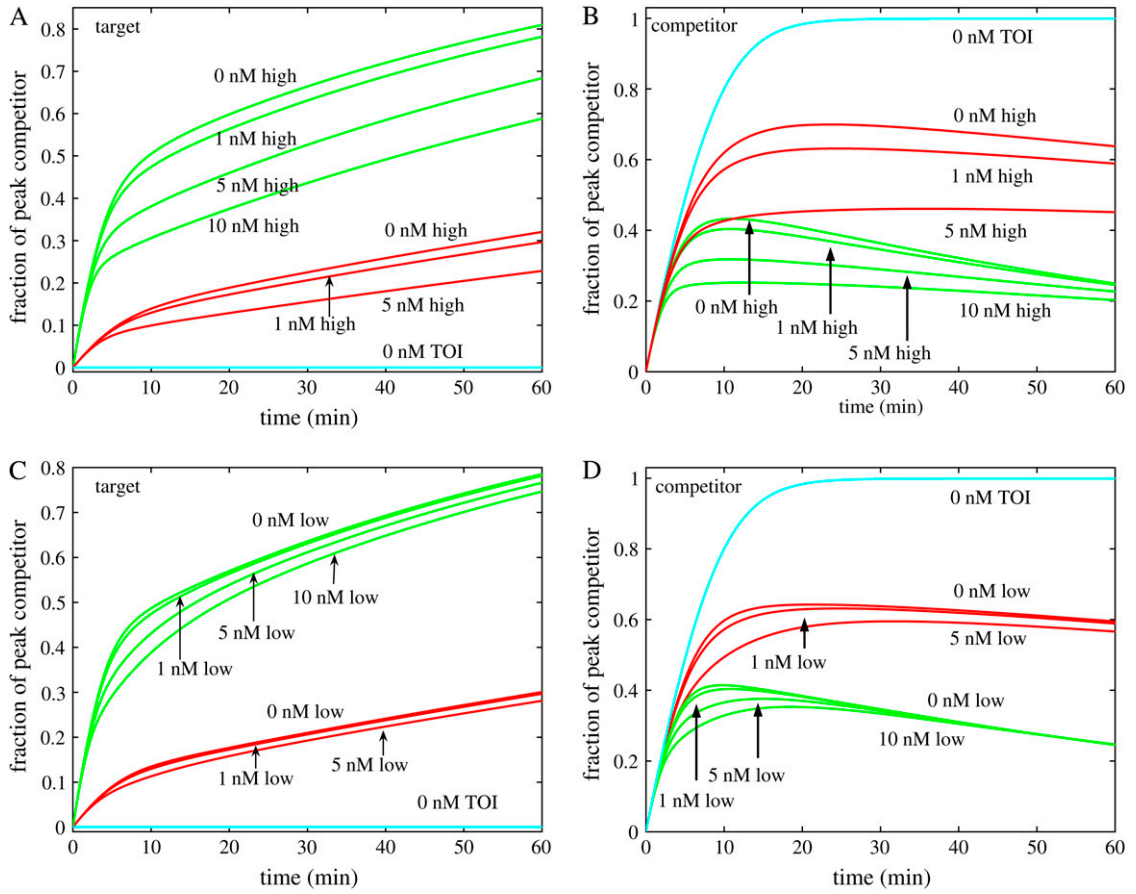

FIGURE 3 Hybridization curves representing the (*A* and *C*) target and (*B* and *D*) competitor kinetics as the concentration of a high (*A* and *B*) or low (*C* and *D*) affinity background is changed from 0 nM to 10 nM. For the red curves the TOI was 1 nM and for the green curves the TOI was 5 nM. The other four background species have a constant concentration of 1 nM and the competitor concentration is 5 nM.

and competitor are modified significantly. The lower-affinity background has less effect; the decrease in the hybridization rates of the target and competitor is less pronounced. However, these results show that even low-affinity species, at high enough concentrations, can still play a role in the signal that is acquired.

The above results motivate a major question for microarray analysis: how many background species (i.e., model components) need to be accounted for during analysis? Fig. 4 shows that accounting for all possible combinations may not be necessary, where the hybridization of the target and competitor are plotted in the presence of two target concentrations and mixtures of five background species (details in Table 1). Using Eqs. 4–6 we have fit these hybridization curves, where Eq. 6 is assumed to be a composite of all remaining species, or in other words, the concentration and rate constants for a third component become apparent. For the fits in Fig. 4, we assume that the rate constants of both the target and competitor are known (via estimated thermodynamic parameters), and that the concentration of the competitor is known. The routine fits the competitor binding curve by adjusting the concentration of the target and the rate constants and concentration of the apparent background. Table 1 shows these fitted values; the fitted target concentration lies within 10% of the actual value used in the simulations.

Several interesting features are demonstrated by applying three-component fits to more complex cases (seven components in our example). First, even though the hybridization curve of the target is not considered in the fitting routine, the reconstructed target kinetics closely matches the simulated kinetics (as shown in Fig. 4 *A*). Second, the kinetics of the apparent background (as represented by the effective dissociation coefficient) does not change significantly with varying background complexity. The effective $k_{d,b}$ values vary by less than a factor of two, and fall within the middle of the dynamic range of the simulated values for the background species; however, the effective concentration of the background consistently tracks the total background concentration.

We have previously shown that it is possible to determine the kinetics of target hybridization indirectly by monitoring the binding of a mismatched competitor in real-time (29); here we have shown that the competitor can be used to assess the influence of the background milieu as well. It is

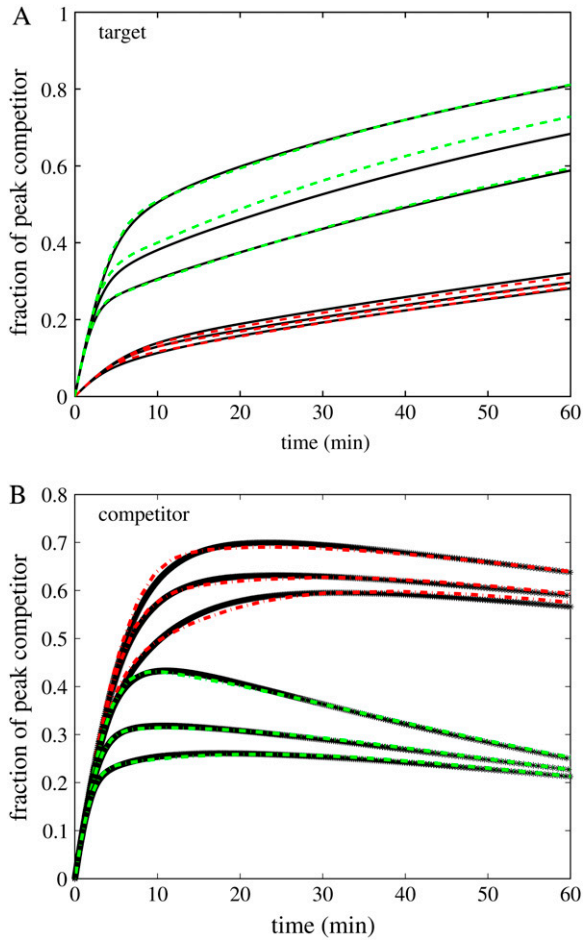

FIGURE 4 Hybridization curves; simulations represented by the black line (taken from previous figures) and fits represented by the dashed lines, representing the (*A*) target and (*B*) competitor kinetics as the concentration of different background species concentrations are changed while the competitor concentration is constant at 5 nM. For the red curves the target of interest was 1.0 nM and for the green curves the target of interest was 5 nM.

important to emphasize that the kinetic behavior of the competitor is very sensitive to the presence of both high-affinity species' target-of-interest (TOI) and lower-affinity species (background) only within a limited range of concentrations. For example, even with scenarios where the apparent affinity of the background is distinctly lower than the affinity of the competitor, increase in the effective background concentration may suppress observation of the competitor binding behavior.

TABLE 1 Fitted target of interest (TOI) concentration and background data from simulation results

Summed background (nM)	TOI actual (nM)	TOI fit (nM)	Back. fit (nM)	Back. k_d (10^{-4} s^{-1})
4.0	1.0	1.0	1.8	15
5.0	1.0	1.1	3.0	11
9.0	1.0	1.1	5.3	14
4.0	5.0	5.0	3.1	11
9.0	5.0	5.3	7.1	11
14.0	5.0	5.5	12	8.8

Values given represent curves shown in Fig. 4 from highest to lowest fraction of peak competitor. The competitor concentration is 5 nM.

Experimental

Experiments were first performed to verify the effect of background on the competitor in the absence of the target. Fig. 5 *A* shows the hybridization curves of the competitor as the concentration of the deletion is increased, while Fig. 5 *B* shows the hybridization of the competitor as the tandem mismatch (TMM) is increased. In both cases, the competitor is not displaced because it has a higher affinity than the two background species. Based on these results, we have also verified that the deletion has a lower affinity than the TMM, but the deletion is still a significant source of background.

Fits of the experimental traces were performed using the three-component approximation described above, with the background concentration and rate constants free parameters, but with known competitor concentration and rate constants, and known target rate constants. In the three-component fit here, an apparent target concentration is obtained even though no target is present in solution. This concentration represents the lower limit of discrimination and is ~10 fM for these experiments. This lower limit can be decreased by either measuring over a longer period of time or by improving the signal/noise ratio of the system.

In a microarray experiment, a researcher is searching for a target in the presence of many other species. Fig. 5 *C* uses two different target concentrations and shows how, as the deletion concentration is increased in the mixture, the competitor hybridization is changed. Additionally, Fig. 5 *D* shows how the competitor hybridization changes as the concentration of the TMM increases. The experimental data were fit using the same procedure described above, verifying that the three-component model works experimentally when a target of interest is present. Table 2 shows that the fits predict target concentrations within 25% of the experimental values. Similar to the result shown in Fig. 5, *A* and *B*, the TMM decreases the hybridization rate of the competitor more than does the deletion, because of its higher relative affinity. It should be noted that at equimolar target and competitor concentration, the maximum value of the competitor (normalized to the maximum value of the competitor alone) is 0.5, so that the effects of background can be evaluated by deviation of the competitor peak below this value.

DISCUSSION AND CONCLUSION

Recently, the kinetics of hybridization of a primary target in the presence of a secondary mismatched species has been investigated using computational (18,20,22,26,36) and experimental (4,28) approaches. While these studies have only

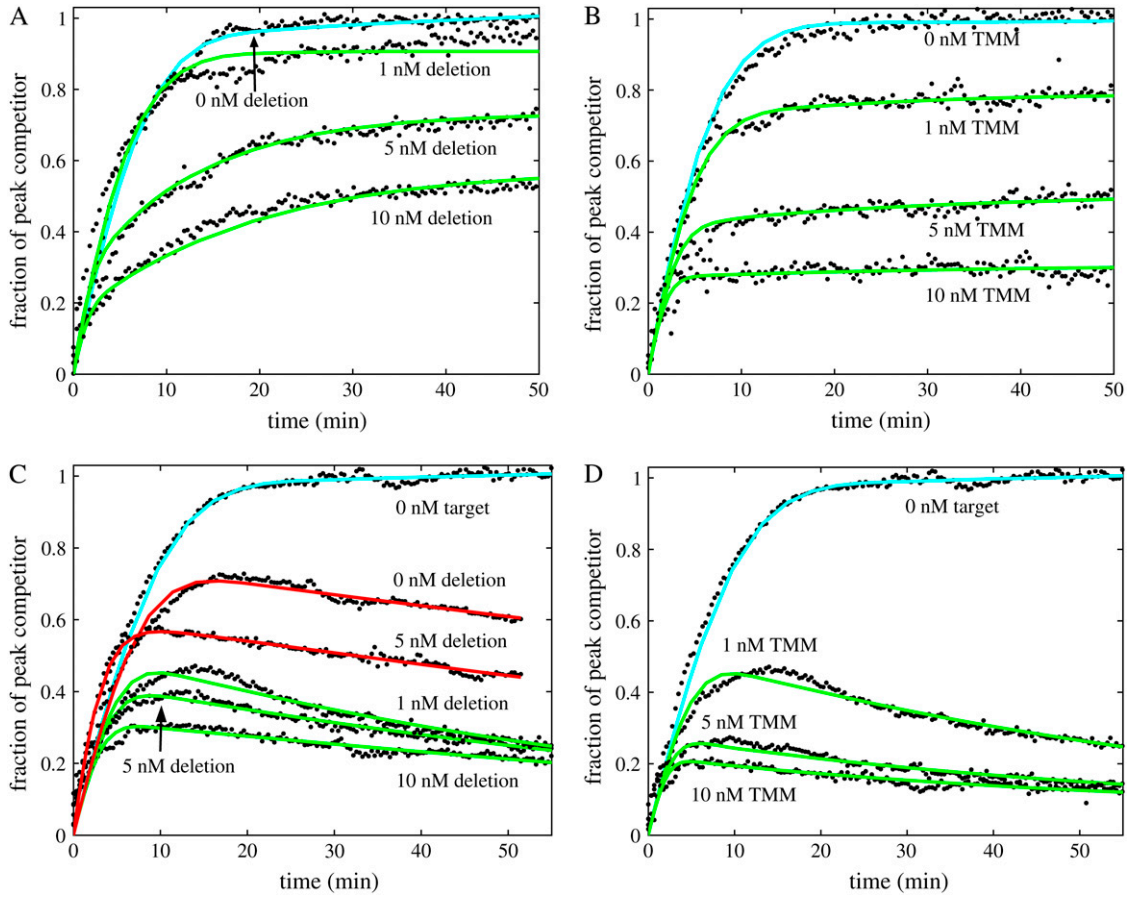

FIGURE 5 Hybridization curves (experimental data represented by *dots* while fits are represented by *solid lines*) representing the competitor kinetics as the concentration of deletion (*A* and *C*, with fixed 1 nM TMM) and TMM (*B* and *D*, with fixed 1 nM deletion) are shifted from 0 nM to 10 nM while the competitor concentration is constant at 5 nM. In panels *C* and *D*, the red curves are for target concentration of 1.6 nM and the green curves are for target concentration 5 nM; target is absent in panels *A* and *B*.

considered the competition between two sequences with a single probe, some features are apparent:

1. The specificity of recognition is controlled by the competitive displacement of the lower-affinity species by the higher-affinity one;
2. The signature of this mechanism is a nonmonotonic growth curve of the lower-affinity species;
3. Depending on the relative concentration and rate constants of the primary and secondary species, the latter may become a major contributor to the observed signal, especially in the transient regime;
4. The presence of the secondary species extends the time to reach equilibrium;
5. The maximum specificity is obtained at equilibrium; and
6. In the absence of the primary target, the secondary species may produce a signal comparable to the primary target alone.

TABLE 2 Fitted target of interest (TOI) concentration and background data from the experimental curves shown in Fig. 5

Deletion (nM)	TMM (nM)	TOI actual (nM)	TOI fit (nM)	Back. fit (nM)	Back. k_d (10^{-4} s^{-1})
0	1	1.6	1.2	0.44	16
5	1	1.6	1.9	1.6	10
1	1	5	5.2	0.65	14
5	1	5	4.9	2.7	9.5
10	1	5	4.8	7.9	8.3
1	5	5	6.2	3.7	10
1	10	5	6.3	12	5.9

The competitor concentration is 5 nM.

These observations were generalized here to the more complex environment in which the interaction among N species (i.e., a target and N–1 background) must be considered, all of varying affinities to a given probe. The fundamental questions are then how the background affects the kinetics of the target hybridization and how the target can be properly quantified given the influence of the background. While analysis and interpretation may seem daunting, we showed that the complex N component system can be reduced to a system of three components (the target plus two effective background components, one of which we term the competitor). We demonstrated the validity of this reductionist

approach by fitting simulated and experimental binding curves of samples with different compositions. This result opens the way to develop new analytical techniques for quantitative analysis. For example, we showed that by analyzing the binding curve of a known secondary target, which we call a competitor, we can evaluate the concentration of a primary target in an unknown sample composition. However, based on this mechanistic analysis, there are some intrinsic limitations in the application of this approach: when the effective concentration of the background is considerably greater than that of competitor, we may not be able to observe the competitor's kinetics due to the limited signal/background in detection.

Our results demonstrate several important advantages of the kinetic analytical approach discussed above. One is that we practically eliminate false positive calls. Indeed, in the absence of primary targets, the competitor binding curves grow monotonically, while in the presence of the primary targets, they display nonmonotonic behavior. Secondly, the detection approach we employed eliminates fluorescent labeling of the sample, because target quantitation is based solely on the binding of the competitor (which itself must be fluorescently labeled). Third, by applying a three-component model to analyze experimental binding curves, we demonstrated expanded dynamic range of quantitations: in our example it was determined to be $\sim 10^6$. Lastly, the time of the experiment is greatly reduced: analysis is performed on transient binding curves, which eliminates requirements of reaching equilibrium.

Admittedly, there is a considerable gap between the simplified model system that we have presented and high-density microarray experiments with biological samples. Our results suggest that, in scaling to more complex systems, hybridization at each spot in the array can be described by a three-component model. However, our model neglects other competing reactions, which also need to be incorporated. Further, proper design of competitor sequences needs to be considered to turn our model into an analytical tool that, in the end, must be validated against experiments of biological significance.

In conclusion, we have studied the kinetics of multiplex hybridization and have suggested that a simplified three-component kinetic model is sufficient to capture the dynamics. In fact, the three-component model provides remarkably good agreement with experimental results. More research needs to be performed to evaluate the limits of the three-component model and its use in novel analysis methods.

The authors are grateful for discussions with A. S. Benight and for comments by the reviewers.

This research was performed within the Center for Microarray Technology, which is supported in part by the Utah Centers of Excellence Program and the University of Utah Technology Commercialization Project. Financial support for J. Bishop has been provided by a National Science Foundation fellowship (NSF No. IGERT:DGE 9987616) and by the Centers of Excellence.

REFERENCES

1. Levicky, R., and A. Horgan. 2005. Physicochemical perspectives on DNA microarray and biosensor technologies. *Trends Biotechnol.* 23: 143–149.
2. Wang, Y., C. Barbacioru, F. Hyland, W. Xiao, K. L. Hunkapiller, J. Blake, F. Chang, C. Gonzalez, L. Zhang, and R. R. Samaha. 2006. Large-scale real-time PCR validation on gene expression measurements from two commercial long-oligonucleotide microarrays. *BMC Genomics.* 7:59.
3. Held, G. A., G. Grinstein, and Y. Tu. 2006. Relationship between gene expression and observed intensities in DNA microarrays—a modeling study. *Nucleic Acids Res.* 34:e70.
4. Fish, D. J., M. T. Horne, R. P. Searles, G. P. Brewood, and A. S. Benight. 2007. Multiplex SNP discrimination. *Biophys. J.* 92:L89–L91.
5. Provenzano, M., and S. Mocellin. 2007. Complementary techniques: validation of gene expression data by quantitative real time PCR. *Adv. Exp. Med. Biol.* 593:66–73.
6. Berrar, D. P., W. Dubitzky, and M. Granzow, editors. 2003. A Practical Approach to Microarray Data Analysis. Kluwer Academic Publishing, New York.
7. Lee, N. H., and A. I. Saeed. 2007. Microarrays: an overview. *Methods Mol. Biol.* 353:265–300.
8. Weis, B. K. 2005. Standardizing global gene expression analysis between laboratories and across platforms. *Nat. Methods.* 2:351–356.
9. Oh, S. J., B. J. Hong, K. Y. Choi, and J. W. Park. 2006. Surface modification for DNA and protein microarrays. *OMICS: J. Integr. Biol.* 10:327–343.
10. Dandy, D. S., P. Wu, and D. W. Grainger. 2007. Array feature size influences nucleic acid surface capture in DNA microarrays. *Proc. Natl. Acad. Sci. USA.* 104:8223–8228.
11. Livshits, M. A., and A. D. Mirzabekov. 1996. Theoretical analysis of the kinetics of DNA hybridization with gel-immobilized oligonucleotides. *Biophys. J.* 71:2795–2801.
12. Chan, V., D. J. Graves, P. Fortina, and S. E. McKenzie. 1997. Absorption and surface diffusion of DNA oligonucleotides at liquid/solid interfaces. *Langmuir.* 13:320–329.
13. Dai, H., M. Meyer, S. Stepaniants, M. Ziman, and R. Stoughton. 2002. Use of hybridization kinetics for differentiating specific from non-specific binding to oligonucleotide microarrays. *Nucleic Acids Res.* 30:e86.
14. Adey, N. B., M. Lei, M. T. Howard, J. D. Jensen, D. A. Mayo, D. L. Butel, S. C. Coffin, T. C. Moyer, D. E. Slade, M. K. Spute, A. M. Hancock, G. T. Eisenhoffer, B. K. Dalley, and M. R. McNeely. 2002. Gains in sensitivity with a device that mixes microarray hybridization solution in a 25-μm-thick chamber. *Anal. Chem.* 74:6413–6417.
15. Erickson, D., X. Liu, U. Krull, and D. Li. 2004. Electrokinetically controlled DNA hybridization microfluidic chip enabling rapid target analysis. *Anal. Chem.* 76:7269–7277.
16. Situma, C., M. Hashimoto, and S. A. Soper. 2006. Merging microfluidics with microarray-based bioassays. *Biomol. Eng.* 23:213–231.
17. Sorokin, N. V., D. Y. Yurasov, A. L. Cherepanov, J. M. Kozhekbaeva, V. R. Chechetkin, O. A. Gran, M. A. Livshits, T. V. Nasedkina, and A. S. Zasedatelev. 2007. Effects of external transport on discrimination between perfect and mismatch duplexes on gel-based oligonucleotide microchips. *J. Biomol. Struct. Dyn.* 24:571–578.
18. Bishop, J., S. Blair, and A. Chagovetz. 2007. Convective flow effects on DNA biosensors. *Biosens. Bioelectron.* 22:2192–2198.
19. Bhanot, G., Y. Louzoun, J. Zhu, and C. DeLisi. 2003. The importance of thermodynamic equilibrium for high throughput gene expression arrays. *Biophys. J.* 84:124–135.
20. Bishop, J., S. Blair, and A. Chagovetz. 2006. A competitive kinetic model of nucleic acid surface hybridization in the presence of point mutants. *Biophys. J.* 90:831–840.
21. Halperin, A., A. Buhot, and E. B. Zhulina. 2006. On the hybridization isotherms of DNA microarrays: the Langmuir model and its extensions. *J. Phys. Condens. Matter.* 18:S463–S490.

22. Horne, M. T., D. J. Fish, and A. S. Benight. 2006. Statistical thermodynamics and kinetics of DNA multiplex hybridization reactions. *Biophys. J.* 91:4133–4153.

23. Halperin, A., A. Buhot, and E. B. Zhulina. 2004. Sensitivity, specificity, and the hybridization isotherms of DNA chips. *Biophys. J.* 86:718–730.

24. Wren, J. D., A. Kulkarni, J. Joslin, R. A. Butow, and R. G. Harold. 2002. Cross-hybridization on PCR-spotted microarrays. *IEEE Eng. Med. Biol.* 21:71–75.

25. Okoniewski, M. J., and C. J. Miller. 2006. Hybridization interactions between probesets in short oligo microarrays lead to spurious correlations. *BMC Bioinformatics.* 7:276.

26. Zhang, Y., D. A. Hammer, and D. J. Graves. 2005. Competitive hybridization kinetics reveals unexpected behavior patterns. *Biophys. J.* 89:2950–2959.

27. Stimpson, D. I., J. V. Hoijer, W. T. Hsieh, C. Jou, J. Gordon, T. Theriault, R. Gamble, and J. D. Baldeschwieler. 1995. Real-time detection of DNA hybridization and melting on oligonucleotide arrays by using optical waveguides. *Proc. Natl. Acad. Sci. USA.* 92:6379–6383.

28. Bishop, J., A. Chagovetz, and S. Blair. 2007. Competitive displacement of DNA during surface hybridization. *Biophys. J.* 92:L10–L12.

29. Bishop, J., A. Chagovetz, and S. Blair. 2007. Competitive displacement: a sensitive and selective method for the detection of unlabeled molecules. *Opt. Express.* 15:4390–4397.

30. Tawa, K., D. Yao, and W. Knoll. 2005. Matching base-pair number dependence of the kinetics of DNA-DNA hybridization studied by surface plasmon fluorescence spectroscopy. *Biosens. Bioelectron.* 21:322–329.

31. Erickson, D., D. Li, and U. Krull. 2003. Modeling of DNA hybridization kinetics for spatially resolved biochips. *Anal. Biochem.* 317: 186–200.

32. Peterson, A. W., L. K. Wolf, and R. M. Georgiadis. 2002. Hybridization of mismatched or partially matched DNA at surfaces. *J. Am. Chem. Soc.* 124:14601–14607.

33. Hagan, M. F., and A. K. Chakraborty. 2004. Hybridization dynamics of surface immobilized DNA. *J. Chem. Phys.* 120:4958–4968.

34. Gao, Y., L. K. Wolf, and R. M. Georgiadis. 2006. Secondary structure effects on DNA hybridization kinetics: a solution versus surface comparison. *Nucleic Acids Res.* 34:3370–3377.

35. Myszka, D. G., X. He, M. Dembo, T. A. Morton, and B. Goldstein. 1998. Extending the range of rate constants available from BIACORE: interpreting mass transport-influenced binding data. *Biophys. J.* 75: 583–594.

36. Chechetkin, V. R. 2007. Two-compartment model for competitive hybridization on molecular biochips. *Phys. Lett. A.* 360:491–494.

37. Sekar, M. M. A., W. Bloch, and P. M. S. John. 2005. Comparative study of sequence-dependent hybridization kinetics in solution and on microspheres. *Nucleic Acids Res.* 33:366–375.